Recent weakening of northern East Asian summer monsoon: A possible response to global warming

Congwen Zhu,[1] Bin Wang,[2] Weihong Qian,[3] and Bo Zhang[4]

Received 2 February 2012; revised 30 March 2012; accepted 30 March 2012; published 1 May 2012.

[1] We investigate the possible causes of the weakening of northern East Asian summer monsoon (EASM) from 1954 to 2010. We found that the decreased intensity of northern EASM as measured by a circulation index (EASMI) is significantly correlated with the increase of the surface air temperature (SAT) averaged over the Lake Baikal region (45°–65°N, 80°–130°E) defined as SATI. Corresponding to increasing SATI, an anomalous low-level anticyclone occurs with northeasterly prevailing over northern East Asia (30°–50°N, 100°–130°E), resulting in a weakened southwesterly monsoon winds and drier climate in this region. Numerical experiments with the community atmosphere model version 3 (CAM3) show that the joint forcing induced by greenhouse gases (GHG), sea surface temperature (SST), solar radiance (SR), and volcano activity (VC) can replicate the observed trend of SATI and its related circulation anomalies, but without GHG forcing the model failed to simulate the warming trend of SATI after 1970s. This implies that the global warming is likely responsible for the local warming around the Lake Baikal, which in turn weakens the northern EASM in recent decades. **Citation:** Zhu, C., B. Wang, W. Qian, and B. Zhang (2012), Recent weakening of northern East Asian summer monsoon: A possible response to global warming, *Geophys. Res. Lett.*, *39*, L09701, doi:10.1029/2012GL051155.

1. Introduction

[2] Evidences suggest that the northern East Asian summer monsoon (EASM) circulation and precipitation has exhibited a downward trend since the late 1970s, which is characterized by weak southwesterly winds over northern East Asia (30°–50°N, 100°–130°E) along with droughts in northern China and floods in Yangtze River Valley [e.g., *Gong and Ho*, 2002; *Yang and Lau*, 2004; *Yu et al.*, 2004; *Xu et al.*, 2006; *Ding et al.*, 2007]. Some suggest the weakening of northern EASM is caused by the upper troposphere cooling over East Asia [*Yu et al.*, 2004], and the cooling possibly caused by the increase of snow cover over the TP and the warming in the tropical Indian and north western Pacific oceans [*Zhao et al.*, 2010]. But some studies suggest that the weakening of northern EASM is mainly caused by the warming of sea surface temperature (SST) over the central and eastern Pacific [e.g., *Yang and Lau*, 2004; *Li et al.*, 2010a]. These studies attributed the downward trend in EASM to lower boundary forcing or internal feedback processes within the climate system. However, the weakening of the northern EASM is concurrently with the recent global warming, and the change of northern EASM may be a part of atmospheric response to the global warming. But, the linkage between the weakening of the northern EASM and global warming is not well understood. For instance, the trends of annul surface air temperature (SAT) suggests that the continental interiors of Asia is one of robust warming region in the past few decades [*Hansen et al.*, 1999, 2006]. This warmer land alone may enhance the EASM in general, but why has the northern EASM exhibited a weakening trend in recent decades? Is it linked to the recent global warming?

[3] In the present study, we try to address these issues on the basis of data analysis and model experiments. The data we used include the GISS (Goddard Institute for Space Study, NASA) global land SAT data [*Hansen et al.*, 1999, 2006], the atmospheric reanalyzed data from the National Centers for Environmental Prediction/National Center for Atmospheric Research (NCEP/NCAR) [*Kalnay et al.*, 1996], and the monthly precipitation data from the global land precipitation reconstruction over land (PREC/L) gridded at 1.0 × 1.0 resolution [*Chen et al.*, 2002]. To avoid the impact of data biases in the sea level pressure (SLP) from the NCEP/NCAR reanalysis (refer to the auxiliary material), the utilized SLP is taken from the Hadley centre version 2 (HadSLP2 [*Allan and Ansell*, 2006]).[1] The study period is from 1954 to 2010 (57 years). The summer is defined as June–August (JJA) mean, and the t-test is applied to test the significance of the results.

2. EASM and the SAT Around the Lake Baikal

[4] To measure the EASM intensity in the present study we adopted a monsoon index (EASMI), which is defined on the basis of land–sea thermal contrasts [*Zhu et al.*, 2005], defined as:

$$\mathrm{EASMI} = (U_{850\mathrm{hPa}} - U_{200\mathrm{hPa}})^*_{(100-130^\circ\mathrm{E},\,0-10^\circ\mathrm{N})} + (SLP_{160^\circ\mathrm{E}} - SLP_{110^\circ\mathrm{E}})^*_{(10-50^\circ\mathrm{N})} \quad (1)$$

where, the '*' indicates the normalized interannual deviation in summer.

[1]Institute of Climate System, Chinese Academy of Meteorological Sciences, Beijing, China.
[2]Department of Meteorology and International Pacific Research Center, School of Ocean and Earth Science and Technology, University of Hawaii at Manoa, Honolulu, Hawaii, USA.
[3]Monsoon and Environment Research Group, School of Physics, Peking University, Beijing, China.
[4]National Meteorological Centre, China Meteorological Administration, Beijing, China.

Corresponding Author: C. Zhu, Institute of Climate System, Chinese Academy of Meteorological Sciences, Beijing 100081, China. (tomzhu@cam.cma.gov.cn)

0094-8276/12/2012GL051155

[1]Auxiliary materials are available in the HTML. doi:10.1029/2012GL051155.

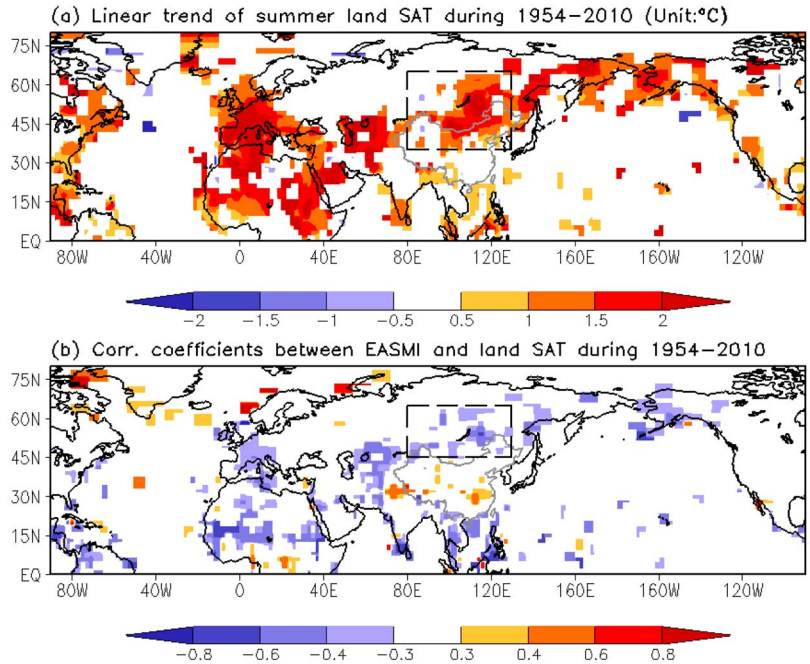

Figure 1. (a) Linear trend of summer land surface air temperature (SAT) which passed the 95 significant tests and (b) the correlation coefficients between the East Asian summer monsoon index (EASMI) and summer SAT in Northern hemisphere continents during 1954–2010. The rectangle regions in Figures 1a and 1b indicate the robust warming region, where the SAT significant negatively correlated with the EASMI and statistically significant at the 5% level, respectively.

[5] Figure 1a shows the linear trend of summer land SAT during 1954–2010. The warming region relevant to the northern EASM is 80°–130°E, 35°–65°N with the *maximum warming* around Lake Baikal, where the warming of SAT in spring plays an important role in reducing the frequency of spring dust storm in north China [*Zhu et al.*, 2008]. Significant positively correlation coefficient (R) is over central China around 30°N, (R is greater than +0.3) and negative correlation (R is less than −0.3) are observed in the region of (45°–65°N, 80°–130°E) with the minimum value of −0.6 centered on Lake Baikal (refer to Figure 1b). To identify the relationship between the EASMI and SAT anomalies around Lake Baikal, we calculated the averaged SAT anomaly index (SATI) over the region of (45°–65°N, 80°–130°E), and present it along with EASMI in Figure 2a. It is clear that the EASMI and the SATI during 1954–2010 show a downward and an upward trend, and both of the trends pass the 99% confidence level. The warming rate of SATI is +0.22°C/decade, which is bigger than any other regions in East Asia. The correlation coefficient between the two indices is −0.36, statistically significant at the 5% level.

[6] The change of summer precipitation is closely associated with the anomalous moisture flux. The SATI-regressed vertically integrated (from 1000 to 300hPa) horizontal moisture transport suggests that the regions from Northeast to central China are dominated by the northeasterly moisture flux anomalies (Figure 2b); it suggests that an increased SATI is associated with a decrease of supply of summer moisture flux in the northwest portion of the northern East Asia (EA). The analysis of linear regression suggests that, a high EASMI is characterized by an anomalous deep low around the Lake Baikal, anomalous southwesterly winds and the enhanced rainfall in northern EA (Figure 2c); meanwhile, the rainfall over the middle-low reaches of Yangtze River valley (Meiyu) is deficient and the climatological southwesterly flow over the subtropical EA (20°–35°N) is weak. Thus, a positive EASMI denotes a stronger-than-normal northern EASM and weaker-than-normal southern EASM. Opposite conditions are associated with a low EASMI. For a more comprehensive discussion of the physical meanings of the EASM circulation indices the readers are referred to *Wang et al.* [2008]. As a result, a weak northern EASM is related to the high pressure around Lake Baikal, where the SAT change in this region, may give rise to the change of EASM intensity.

3. How Does Warming Around the Lake Baikal Affect EASM?

[7] To understand the SATI-related vertical structure of meridional EASM circulation anomalies, we present the height-latitude cross-sections of SATI-regressed fields on air temperature, geopotential height (GPH), zonal wind, and wind speed along 115°E from 1000hPa to 10hPa (Figure 3). It is found that the SATI-regressed air temperature exhibits a significantly reversed pattern between the lower and upper atmosphere north of 40°N, associated with the change of SATI (Figure 3a). The significant positive correlations with the warming trend in the air temperature occur in the lower troposphere below 300hPa and between 40°N and 75°N, and corresponding negative correlations with the cooling trend at the upper levels, but a weak cooling tone related to the change of SATI is observed extending from upper level to the lower level and appearing in the region of Yangtze River valley around 30°N. This results in a cooling trend in the upper troposphere, which agrees well with the past study [*Yu et al.*, 2004]. A robust positive correlation with enhanced GPH appears in the region north of 30°N, with the maximum center at 300hPa, corresponding to the robust warming in the

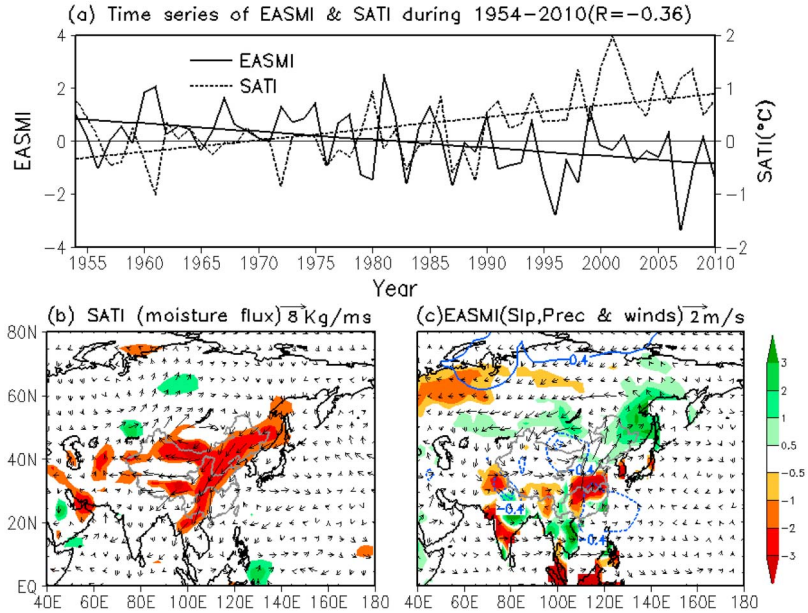

Figure 2. (a) The anomalies and linear trends of East Asian summer monsoon index (EASMI, dashed line) and the surface air temperature index (SATI, solid line, in units of °C), averaged in the region of 45°–65°N, 80°–130°E around Lake Baikal during 1954–2010. (b) The summer SATI-regressed vertical integrated moisture flux from 1000 to 300hPa during 1954–2006 (unit:kg·m^{-1}·s^{-1}), and (c) the EASMI-regressed SLP (blue contours), precipitation (shaded) and wind field at 850hPa,. The color shaded areas in Figure 2b indicates the statistically significant correlation coefficients between SATI and the magnitude of moisture flux, and the EASMI-regressed summer precipitation (unit: mm day^{-1}) derived from PREC/L data in Figure 2c.

air temperature field around 60°N (Figure 3b). The anomalous wind field exhibits a "sandwich" pattern from north to south, with enhanced westerly anomalies in the regions of 60°–75°N, suppressed westerly jet stream in 30°–50N, and enhanced westerly south of 30°N in the troposphere below 100hPa (Figure 3c). The wind speed shows a similar anomalous pattern (Figure 3d). Similar regressed fields can also be observed along 100°E and 120°E (figures are not shown).

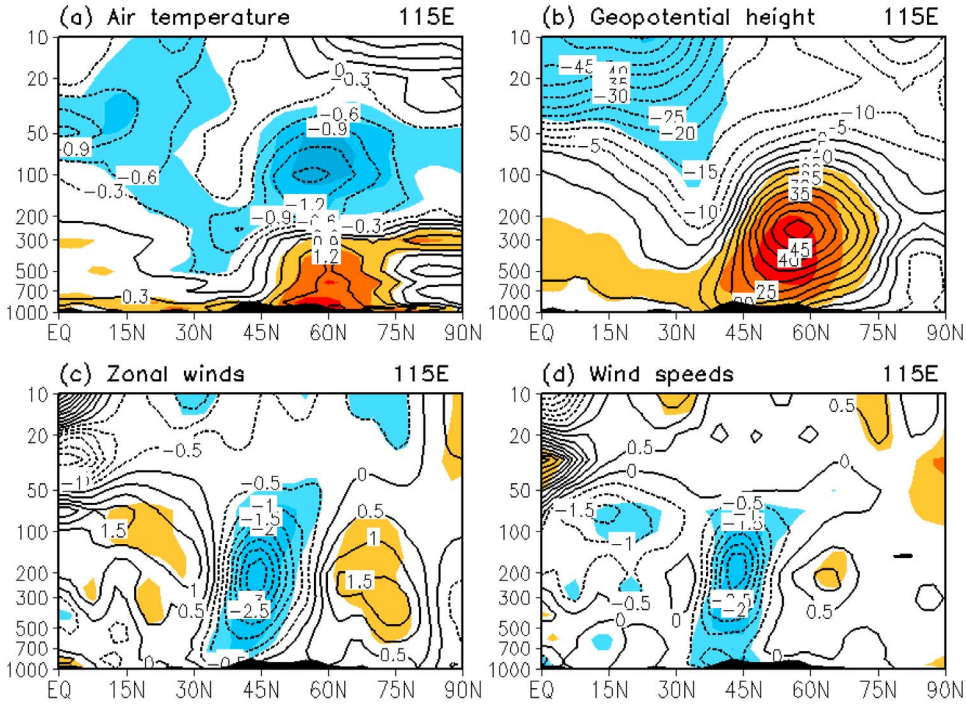

Figure 3. Height-latitude section of summer SATI-regressed (a) air temperature, (b) geopotential height (GPH), (c) zonal wind, and (d) wind speeds along 115°E during 1954–2010. The correlation coefficients statistically significant at the 5% level are shaded. The black shading shows topography.

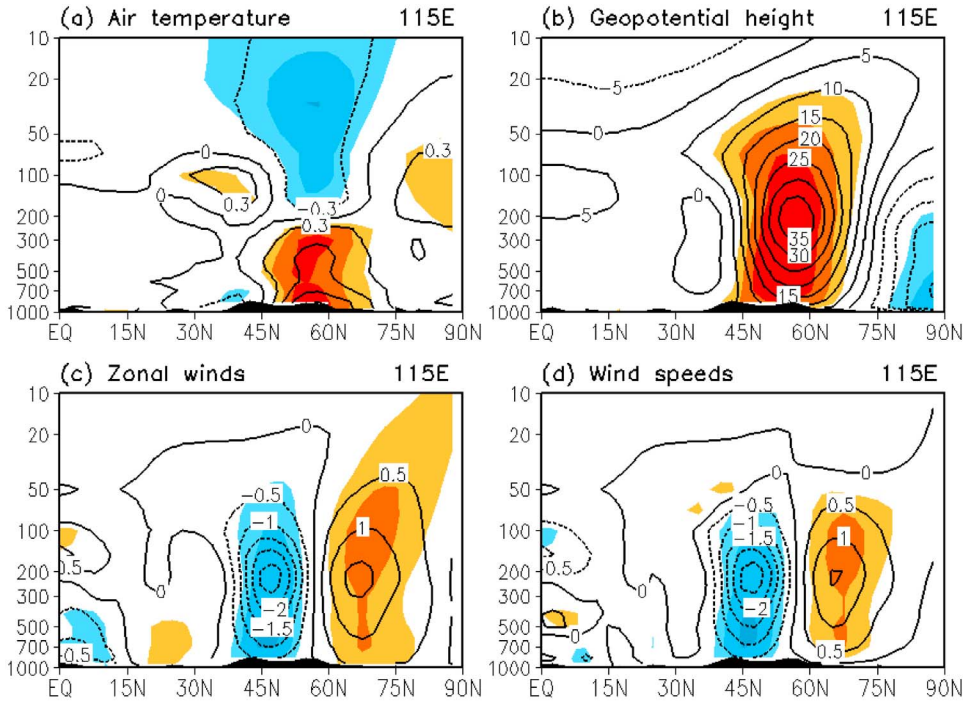

Figure 4. Height-latitude section of model-simulated summer SATI-regressed (a) air temperature, (b) GPH, (c) zonal winds, and (d) wind speeds along 115°E in the model control run during 1954–1999. The correlation coefficients statistically significant at the 5% level are shaded. The black shading shows topography.

Although the SATI exhibits a warming trend in the past decades, its associated air temperature in the upper troposphere shows a reversed trend between troposphere and lower stratosphere north of 40°N over the latitudes of East Asian continent due to the static equilibrium and the vertical mass conservation.

[8] Previous studies suggest that the warming in the Lake Baikal may results in the decrease of meridional air temperature gradient and westerly jet stream over North East Asia, generates a negative vortex, and enhances a warmer anticyclone anomaly over the East Asian continent due to the thermal wind theory [*Li et al.*, 2010b; *Sun et al.*, 2010; *Xu et al.*, 2011]. The northeasterly winds anomalies prevail in the east of anticyclone, and directly weaken the northern EASM as we have seen in Figure 3.

4. What Has Caused the Warming Around the Lake Baikal?

[9] It suggests that the recent warming in North Asian sub-continent regions (NAS, 40°E–180°, 50°–70°N) is likely caused by the increase of well-mixed greenhouse gases (GHG) since the late of 1970s [see *Hegerl et al.*, 2007, Figure 9.12]. However, the observed change of SATI contains both unforced natural variability and anthropogenic forcing. To address the different impacts of natural and anthropogenic forcing on the SATI, the NCAR Community Atmosphere Model version 3 (CAM3), with resolution of T42L18 was applied in present study. The CAM3 includes major modifications to the parameterizations of moist processes, radiation processes, and aerosols. These changes have improved simulations of land surface temperatures [*Collins et al.*, 2006]. In addition, this model can better simulate the seasonal march of EASM and resemble the SAT and rainfall pattern over East Asia (figures are not shown).

[10] We considered the anthropogenic forcing of greenhouse gases (GHG), natural forcing of solar radiation (SR), and volcanic activity (VC) as the main external factors and the sea surface temperature (SST) as the boundary forcing for the atmosphere. To possibly isolate the impacts of these factors, in a control run, we have forced the model with observed GHG, SST, SR, and VC together starting from January of 1900, and integrated the model for 100 years during 20-century (1900–1999). Adaptation of SST forcing makes the long term simulation differs from a free coupled run, in which decadal and interannual variation cannot be compared with observations. However, since SST forcing contains the signature of the external forcing, to some extent a spurious redundant forcing exists. It is argued that this would not fundamentally prevent examination of the continental surface air temperature response to the GHG and other external forcing. In the four parallel sensitivity runs, we subsequently fixed one of the GHG, SST, SR, and VC by their climatology, and replaced the rest three factors by observed values, respectively. Therefore, the control run indicates the model simulation jointly induced by GHG, SST, SR and VC, and the model sensitivity runs denote the possible impact of each of the four factors on the atmosphere (i.e., without the change of GHG, SST, SR, and VC, respectively). We applied the outputs of model control run in the last 46 years (1954–1999) to verify the observed results shown in Figure 3. The model-simulated SATI, derived from the control and four sensitivity runs are calculated to evaluate their possible different impacts.

[11] Figure 4a shows the height-latitude cross-section of model SATI-regressed air temperature along 115°E from

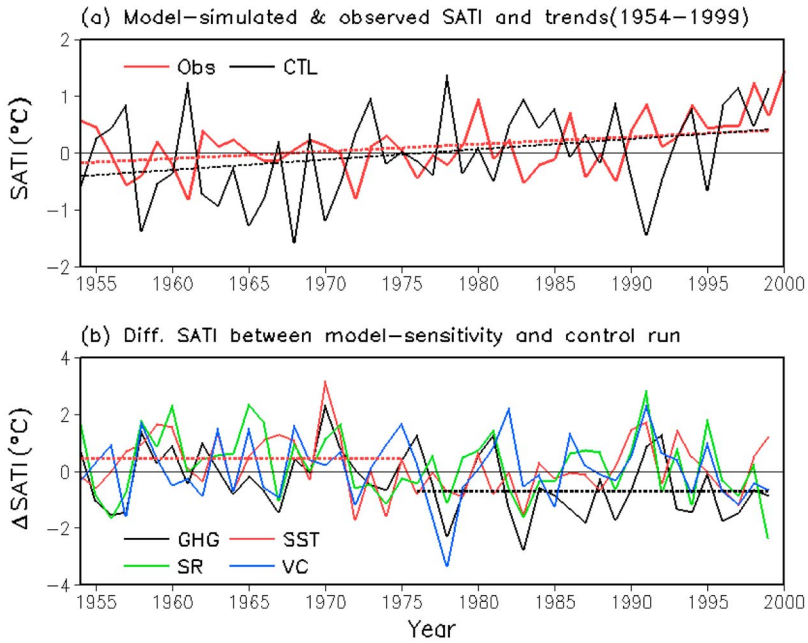

Figure 5. (a) The observed and model-simulated SATI derived from the control (CTL) run during 1954–1999 (unit: °C). the dotted red and black indicates the linear trend of observed and model-simulated SATI, respectively. (b) The difference of SATI between the model control and sensitivity run (sensitivity minus control run) during 1954-1999 without the forcing of greenhouse gases (GHG), sea surface temperature (SST), solar radiation (SR), and volcanic activity (VC) run, respectively. The dotted red and black line indicate the averaged difference of SATI during 1954–1975 and 1976–1999 for the model sensitivity run without forcing of SST and GHG, respectively.

1000hPa to 10hPa in the control run. It is evident that the relationship between the SATI-related air temperature in the lower and upper atmosphere are well simulated by the model north of 40°N, but the model failed to simulate the cooling at the lower atmosphere around 30°N. The SATI-regressed GPH exhibit the positive anomalies along 115°E from 1000hPa to 10hPa in the model control run (Figure 4b), the model SATI-regressed zonal winds and wind speed fields also resemble the observations to the north of 40°N shown in Figures 4c and 4d. Therefore, the SATI-regressed anomalous circulation pattern exhibits a similar structure with the observation shown in Figure 3. The results of model control experiment suggest that a warmer anticyclone anomaly at the lower atmosphere around Lake Baikal is closely linked to the increase of SATI in this region.

[12] Figure 5a shows the time series of observed and the model-simulated SATI anomalies and its linear trends in the control run during 1954–1999. It is found that the model-simulated SATI exhibits a warming trend during 1954–1999, but it can hardly resemble the interannual variability of the observed counterpart, and it even exhibits a weak negative correlation coefficient of −0.12. The model-simulated warming rate of SATI is about +0.17°C/decade, which is greater than the observed rate of +0.12°C during 1954–1999. Figure 5b shows the difference of SATI between the model control run and the four sensitivity runs (sensitivity minus control run), respectively. It is found that the model-simulated SATI without forcing of SST, SR, and VC is higher than that of model control run before 1976, the difference of SATI averaged during 1954–1975 is +0.45°C, +0.43°C and +0.23°C, respectively. However, the SATI anomaly without GHG forcing exhibits a significant downward trend relative to the control run with a cooling rate of −0.2°C/decade during 1954–1999. The averaged SATI anomaly during 1976–1999 is −0.7°C, it is much lower than any other model sensitivity run. Therefore, the GHG may play the most important role in increasing SATI, such a result agrees with the previous study [*Hegerl et al.*, 2007].

5. Summary

[13] In the present study, we examined the weakening of the northern EASM and its possible causes during 1954–2010. We found the EASM index (EASMI) is significantly correlated with the increase of surface air temperature index (SATI) averaged around Lake Baikal region of 80°E–130°E, 45°N–65°N, where the summer SATI-regressed air temperature anomalies over East Asian continent shows a significantly reversed pattern between the lower and upper atmosphere to the north of 40°N, associated with a anomalous anticyclone in this region. Therefore, corresponding to the increase of SATI over the Lake Baikal, the low-level anomalous northeasterlies prevail in the northern East Asia (30°–50°N, 100°–130°E), and results in the weakening of the northern EASM and summer moisture supply.

[14] Numerical experiments with CAM3 shows that the forcing jointly induced by greenhouse gases (GHG), sea surface temperature (SST), solar radiation (SR), and volcano activity (VC) can reproduce the warming trend of SATI during 1954–1999. The differences of SATI between model sensitivity and control run suggests that the model-simulated SATI without GHG exhibits a significant downward trend with a cooling rate of −0.2°C/decade, and it is much lower than any other cases of model sensitivity run after 1976, implying that the global warming associated with the increase of GHG is more likely responsible for the warming

around Lake Baikal and the weakening of the northern EASM in the recent decades. More models' numerical experiments are needed to confirm the model results here.

[15] **Acknowledgments.** The author acknowledges the anonymous reviewers for their helpful comments and suggestions. This study is jointly supported by the China NSF (90711003, 40921003),the key program of 2010Z003 of CAMS, and the "Strategic Priority Research Program - Climate Change: Carbon Budget and Relevant Issues" of the Chinese Academy of Sciences (grant XDA05090400). BW acknowledges the supports from NOAA Climate Test Bed project and the Global Research Laboratory (GRL) program, which is sponsored by National Research Foundation of Korea grant 2100-0021927.

[16] The Editor thanks the two anonymous reviewers for assisting with the evaluation of this paper.

References

Allan, R., and T. Ansell (2006), A new globally complete monthly historical gridded mean sea level pressure dataset (HadSLP2): 1850–2004, *J. Clim.*, *19*(22), 5816–5842, doi:10.1175/JCLI3937.1.

Chen, M. Y., et al. (2002), Global land precipitation: A 50-yr monthly analysis based on gauge observations, *J. Hydrometeorol.*, *3*, 249–266, doi:10.1175/1525-7541(2002)003<0249:GLPAYM>2.0.CO;2.

Collins, W. D., et al. (2006), The formulation and atmospheric simulation of the community atmosphere model version 3(CAM3), *J. Clim.*, *19*, 2144–2161, doi:10.1175/JCLI3760.1.

Ding, Y., Z. Wang, and Y. Sun (2007), Inter-decadal variation of the summer precipitation in east China and its association with decreasing Asian summer monsoon. Part I: Observed evidences, *Int. J. Climatol.*, *28*, 1139–1161, doi:10.1002/joc.1615.

Gong, D.-Y., and C.-H. Ho (2002), Shift in the summer rainfall over the Yangtze River valley in the late 1970s, *Geophys. Res. Lett.*, *29*(10), 1436, doi:10.1029/2001GL014523.

Hansen, J., R. Ruedy, J. Glascoe, and M. Sato (1999), GISS analysis of surface temperature change, *J. Geophys. Res.*, *104*, 30,997–31,022, doi:10.1029/1999JD900835.

Hansen, J., et al. (2006), Global temperature change, *Proc. Natl. Acad. Sci. U. S. A.*, *103*, 14,288–14,293, doi:10.1073/pnas.0606291103.

Hegerl, G. C. et al. (2007), Understanding and attributing climate change, in *Climate Change 2007: The Physical Science Basis. Contribution of Working Group I to the Fourth Assessment Report of the Intergovernmental Panel on Climate Change*, edited by S. Solomon et al., pp. 663–745, Cambridge Univ. Press, Cambridge, U. K.

Kalnay, E., et al. (1996), The NCEP/NCAR 40-year reanalysis project, *Bull. Am. Meteorol. Soc.*, *77*, 437–471, doi:10.1175/1520-0477(1996)077<0437:TNYRP>2.0.CO;2.

Li, H., et al. (2010a), Responses of East Asian summer monsoon to historical SST and atmospheric forcing during 1950–2000, *Clim. Dyn.*, *34*, 501–514, doi:10.1007/s00382-008-0482-7.

Li, J., Z. Wu, Z. Jiang, and J. He (2010b), Can global warming strengthen the East Asian summer monsoon?, *J. Clim.*, *23*, 6696–6705, doi:10.1175/2010JCLI3434.1.

Sun, Y., Y. Ding, and A. Dai (2010), Changing links between South Asian summer monsoon circulation and tropospheric land-sea thermal contrasts under a warming scenario, *Geophys. Res. Lett.*, *37*, L02704, doi:10.1029/2009GL041662.

Wang, B., Z. Wu, J. Li, J. Liu, C.-P. Chang, Y. Ding, and G.-X. Wu (2008), How to measure the strength of the East Asian summer monsoon?, *J. Clim.*, *21*, 4449–4463, doi:10.1175/2008JCLI2183.1.

Xu, K., C. Zhu, and J. He (2011), Impact of the surface air temperature warming around Lake Baikal on trend of summer precipitation in north China in the past 50 years, *Chin. J. Plateau Meteorol.*, *30*(2), 309–317.

Xu, M., C.-P. Chang, C. Fu, Y. Qi, A. Robock, D. Robinson, and H. Zhang (2006), Steady decline of East Asian monsoon winds, 1969–2000: Evidence from direct ground measurements of wind speed, *J. Geophys. Res.*, *111*, D24111, doi:10.1029/2006JD007337.

Yang, F., and K.-M. Lau (2004), Trend and variability of China precipitation in spring and summer: Linkage to sea-surface temperatures, *Int. J. Climatol.*, *24*, 1625–1644, doi:10.1002/joc.1094.

Yu, R., B. Wang, and T. Zhou (2004), Tropospheric cooling and summer monsoon weakening trend over East Asia, *Geophys. Res. Lett.*, *31*, L22212, doi:10.1029/2004GL021270.

Zhao, P., S. Yang, and R. Yu (2010), Long-term changes in rainfall over Eastern China and large-scale atmospheric circulation associated with recent global warming, *J. Clim.*, *23*, 1544–1562, doi:10.1175/2009JCLI2660.1.

Zhu, C., W.-S. Lee, H. Kang, and C.-K. Park (2005), A proper monsoon index for seasonal and interannual variations of the East Asian monsoon, *Geophys. Res. Lett.*, *32*, L02811, doi:10.1029/2004GL021295.

Zhu, C., B. Wang, and W. Qian (2008), Why do dust storms decrease in northern China concurrently with the recent global warming?, *Geophys. Res. Lett.*, *35*, L18702, doi:10.1029/2008GL034886.